Characterization of Thin Reservoirs of Linch area, Cambay Basin using Complex Trace Transform enhancing Temporal Resolution of Seismic Data

Vivek Kumar Singh, P. K. Chaudhuri, GEOPIC, ONGC India, Kamal, IIT Roorkee*
vivekrpsingh@gmail.com

Keywords

Thin bed, Complex trace, Temporal resolution

Summary

In the last few decades, the interest in thin hydrocarbon reservoirs has grown progressively justifying the great effort spent on developing techniques for quantitative interpretation of thin bed seismic response. As the exploration matures in most of the category-I basins of India, focus is gradually shifting towards delineation of thin stratigraphic reservoirs. Many a times it is difficult to precisely estimate the vertical and lateral extensions of a significant portion of discovered hydrocarbon reservoirs due to the thin layer effect.

In pursuance of these objectives, a relatively recent and innovative approach of Complex trace transform has been attempted for improving the thin bed delineation from seismic data in Linch area of Cambay Basin. In this area, the sands which are dispersed especially within Older Cambay Shale (OCS) are thin and discrete in nature and are not properly discernible on seismic, in particularly at deeper levels. Results of the study validate the discrete and thin beds within LU-I & LU-III sand units encountered in the wells.

Introduction

The interest in thin hydrocarbon reservoirs has grown progressively justifying enhanced effort to develop new techniques for quantitative interpretation of thin bed seismic response. The detection and resolution of reflections from thin layers are major problems in reflection seismic. Difficulty in precise estimate of the vertical and lateral extensions of a discovered thin hydrocarbon reservoirs leads to under or over estimation of reserves.

In Linch area of Cambay basin , the sands which are dispersed especially within Older Cambay Shale (OCS) are thin and discrete in nature and are not properly discernible on seismic, in particularly at deeper levels; some of these sands hold commercial oil and gas. Even within shallower Kalol formation most of the sands are quite thin to be delineated by conventional seismic interpretation. A small part of Linch area comprising of 6 wells, namely, LN-A, LN-B, LN-C, LN-D, LN-E, LN-F has been taken up for this study (Fig.1).

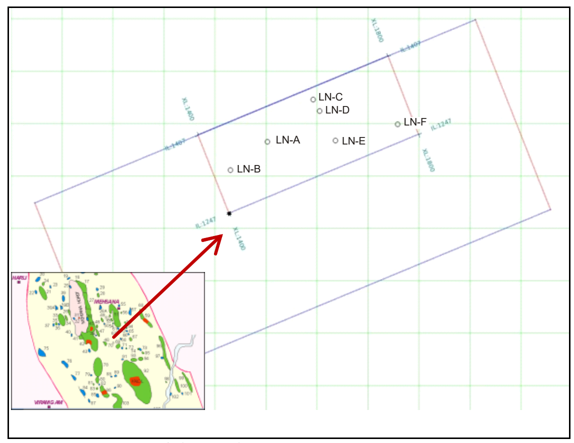

Fig. 1: Base map of the study area.

Log characteristics and corresponding seismic response for well LN-A shows that the sands which are dispersed especially within Older Cambay Shale (OCS) are thin and discrete in nature and are not properly discernible on seismic, in particularly at deeper levels. Sands being thin, the seismic response is of composite nature arising out of several sand-shale alterations (Fig.2).

Rockphysics analysis based on well logs indicates the porous sands to be having impedance within the range of shale impedance, but mostly towards higher order (Fig.3). Inversion using conventional approach turns out to be of no practical use. In this study we have investigated the approach for thin reservoir evaluation through complex trace transform (CTT) method, results of which has been subjected to inversion.

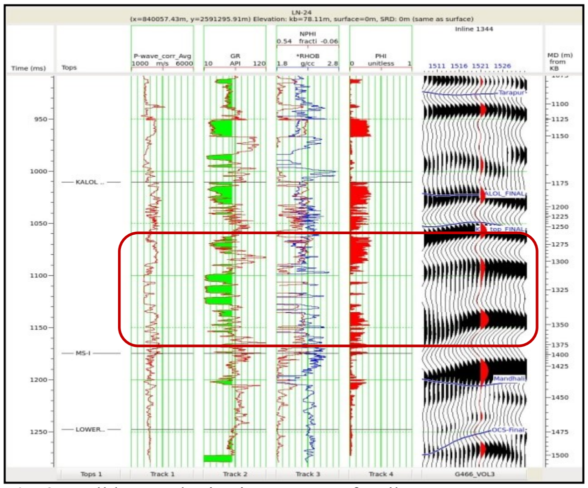

Fig. 2: Well logs and seismic response of well LN-A.

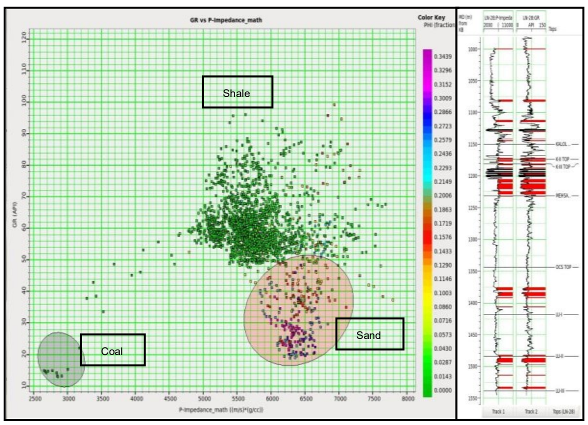

Fig. 3: Cross plot of P-imp vs GR, colored by Porosity for well LN-B.

Methodology

Complex-trace transformation (CTT) that uses complex-trace envelope and normalized phase traces to improve the temporal resolution and to increase S/N of stacked seismic data is adopted here. We can represent seismic traces using their envelopes and instantaneous phases obtained by the Hilbert transform (Hakan Karsli, 2006). This method reduces the amplitudes of the low-frequency components of the envelope, while preserving the phase information. Applications on synthetic data show that the method is capable of reducing the amplitudes and temporal widths of the side lobes of the input wavelets, and hence, the spectral bandwidth of the input seismic data is enhanced, resulting in an improvement in the signal-to-noise ratio. Workflow is given below.

Workflow

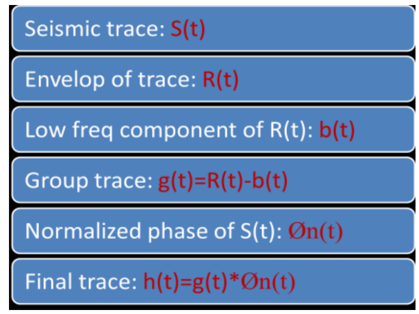

Using amplitude and phase information, seismic traces can be expressed as

$S(t) = R(t)\cos\Theta(t)$

where R(t) is the envelope and $\Theta(t)$ is the time-dependent phase information of the seismic trace, both of which can be determined from the seismic trace by Hilbert transform.

This can be re-written as

$S(t) = R(t)\Theta n(t)$

where $\Theta n(t)$ is normalized phase or the cosine of the instantaneous phase $\Theta(t)$ and can be expressed as

$\Theta n(t) = S(t)/R(t)$.

The envelope is a positive valued trace; however, one can convert the envelope trace to an oscillating time series with both positive and negative values similar to the input seismic trace. To do this, the low-frequency component b(t) is computed, for instance as a running average within a given-time window, Tw, and subtracted from R(t) to get $g(t)= R(t) - b(t)$ and this is the so-called group trace.

Seismic traces can be decomposed into their normalized phase and group trace components and can then be reconstructed to compare with the input seismic trace as follows

$h(t)= g(t)\,\Theta n(t)$, for $g(t) \geq 0$

and $h(t)= 0$, for $g(t) \leq 0$.

These two equations express the reconstruction of the final seismic traces using their normalized phase and group traces. The zero and negative parts of the group traces correspond to side lobes and low-frequency random-noise components of the seismic data, because the group trace is obtained by subtracting the low-frequency component from the envelope trace. Therefore, the omission of zero or negative values in the group trace can improve the temporal resolution and decrease the low-frequency random noise level in the seismic data. Thus, this process improves the temporal resolution because the amplitudes of the side lobes are reduced.

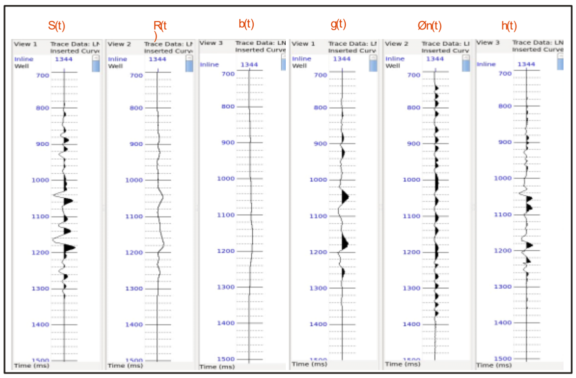

Fig. 4: Application of CTT workflow on a single seismic trace.

Experimentation

First a seismic trace S(t) was taken from 3D seismic data at well location LN-A for experimentation of CTT method. As per the work flow first envelope R(t) of seismic trace is calculated and then its low frequency component b(t) is calculated. Group trace g(t) is calculated by subtracting b(t) from R(t). Normalized phase ϴn(t) of input seismic is also calculated. Finally CTT output trace h(t) is calculated by multiplying g(t) and ϴn(t). Step by step output of this experimentation process is shown in Fig.4. Comparison of input and output trace is shown in Fig.5 with trace repetitions for better display. It shows the significant improvement in resolvability in whole trace. Fig.6 shows the amplitude spectrum of input trace (above) and output trace (below). The bandwidth of output trace is increased significantly in comparison to bandwidth of input trace, which in turns helps in resolving the thin beds. Same exercise has been repeated at other well locations also.

Application on real data

After successful experimentation on single trace, the CTT method was applied on a seismic section. An IL section passing through well LN-A has been taken as input section. To test the suitable gate of running average time windows (Tw), CTT method was applied on input section with different Tw gates. The CTT output sections with Tw of 200ms and 300ms are shown in Fig.7.

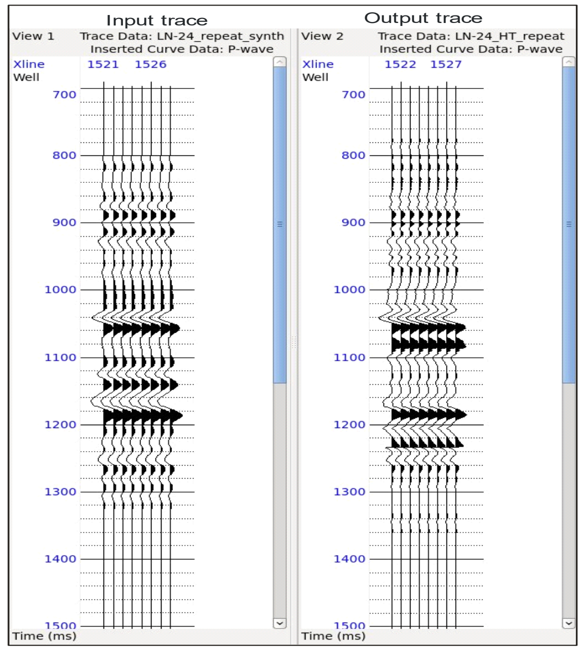

Fig. 5: Comparison of input seismic trace and its CTT output trace.

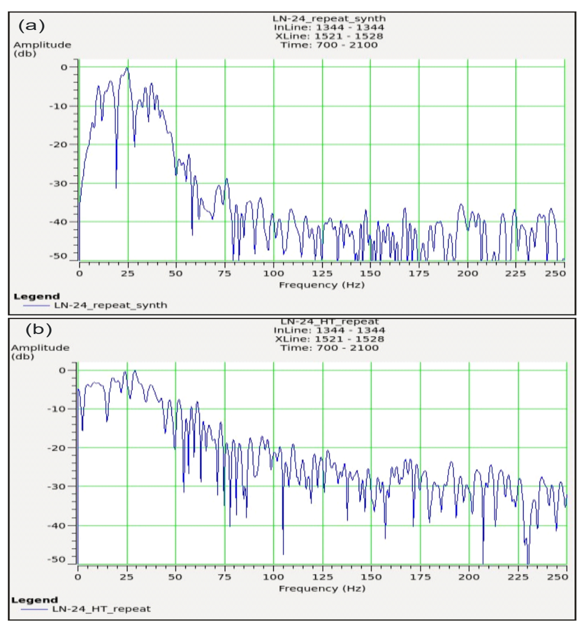

Fig. 6: (a) Amplitude spectrum of input trace and (b) output trace

CTT output with Tw of 300ms is found suitable for this dataset. Amplitude spectrum of input section and output section is shown in Fig.8. After application of CTT method, the frequency bandwidth of input section is significantly increased from range of 8-42 Hz to 0-65 Hz at -12 db level, within zone of inetrest.

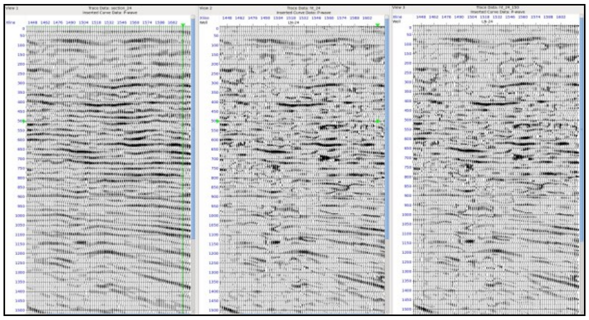

Fig. 7: Input seismic section (left), CTT section with Tw=200ms (middle), CTT section with Tw=300ms (right).

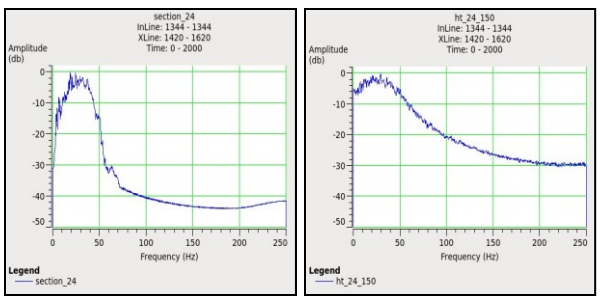

Fig. 8: Amplitude spectrum of input seismic section (left) and CTT section (right).

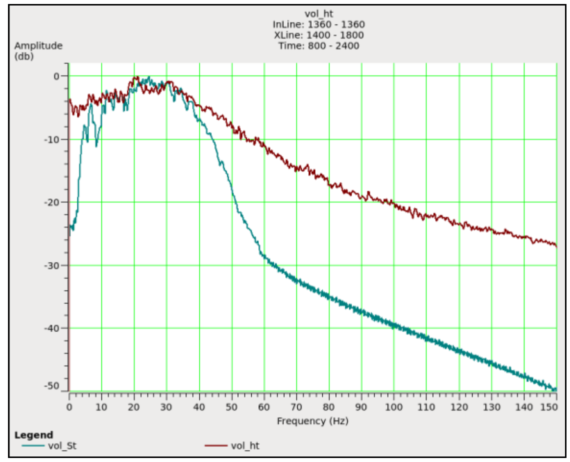

Fig. 10: Amplitude spectrum of original seismic and CTT seismic volume.

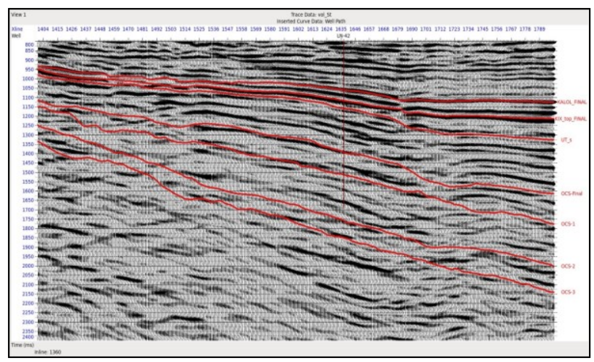

Fig. 11: Seismic section (IL-1360) overlain with different horizons used for generating attribute slices.

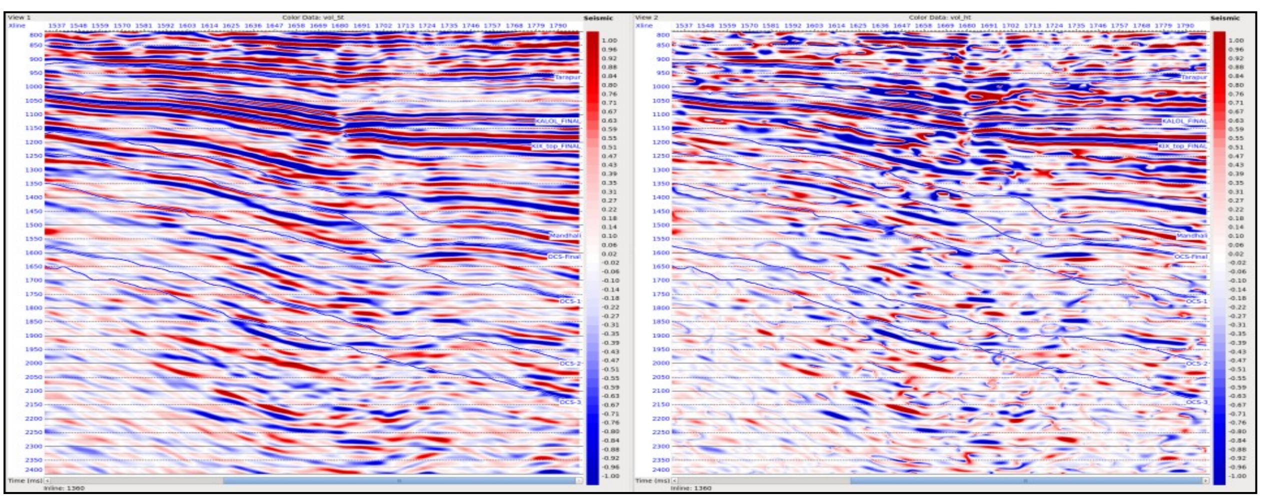

Fig. 9: Seismic section (left) and CTT section (right) passing through IL-A.

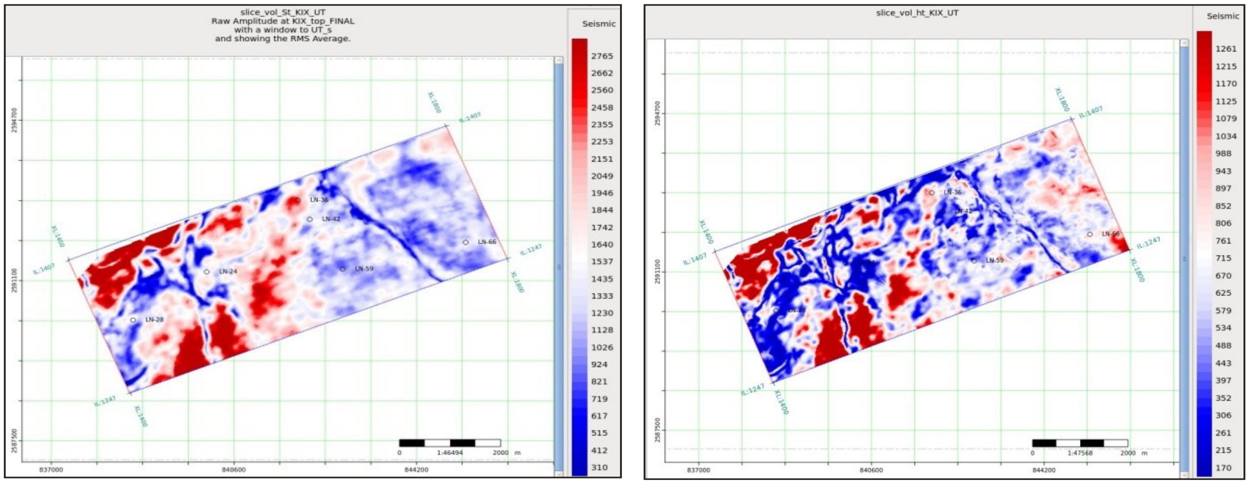

Fig. 12: Slice of rms amplitude of original seismic (left) and CTT seismic (right) calculated within window of KIX and UT.

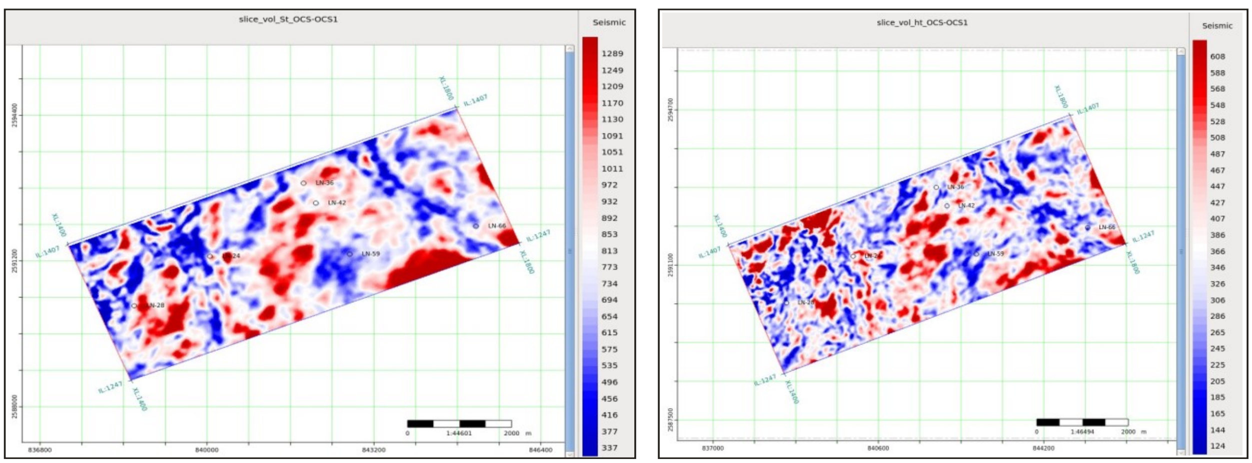

Fig. 13: Slice of rms amplitude of original seismic (left) and CTT seismic (right) calculated within window of OCS and OCS1.

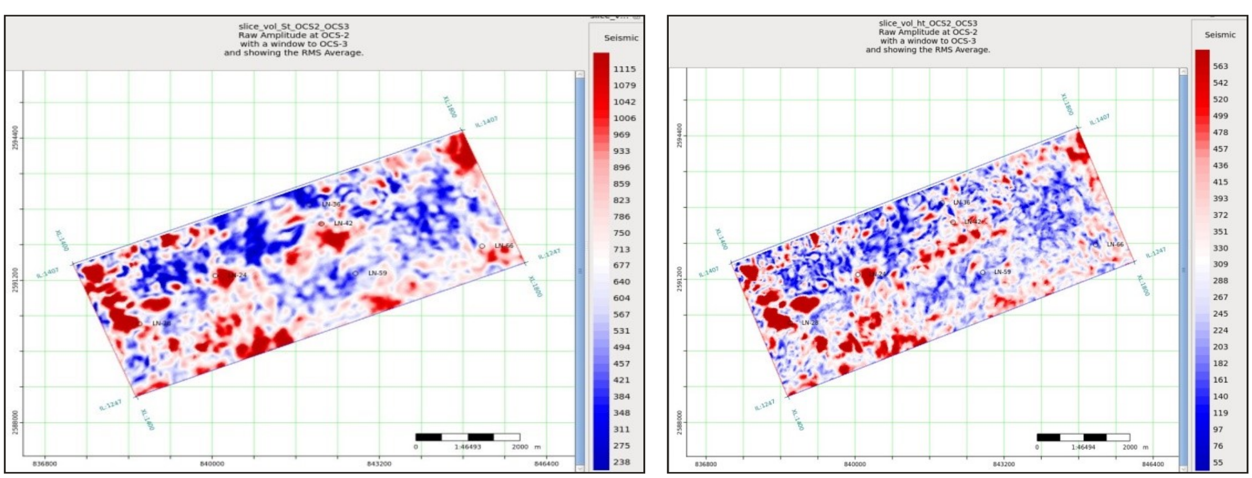

Fig. 14: Slice of rms amplitude of original seismic (left) and CTT seismic (right) calculated within window of OCS2 and OCS3.

Once the CTT method is tested on a trace and on a section, it is applied on 3D seismic volume. A seismic section passing through IL-A and its corresponding CTT output is shown in Fig.9. Comparison of amplitude spectrums of input seismic volume and CTT output volume is shown in Fig.10. Here also a significant increase in frequency bandwidth of input data can be observed.

To see the improvement in resolvability of seismic data, attribute slices have been generated at different horizon levels. A seismic section overlain with different horizons used for generating attribute slices is shown in Fig.11. Slices of rms amplitude are generated between KIX & UT, OCS & OCS-1, and OCS-2 & OCS-3 levels for both original as well as CTT seismic. Slices of rms amplitude generated for above mentioned windows, using original seismic as well as CTT seismic are shown in Fig.12, Fig.13, & Fig.14.

Inversion

Post stack seismic inversion was carried out for both, original as well as CTT seismic volume. A section of inverted P-impedance overlain with P-imp log along an arbitrary line passing through all wells is shown in Fig.15. Also, a section of inverted P-impedance of CTT seismic overlain with P-imp log along same line is shown in Fig.16. The inverted P-imp section of CTT seismic is able to discriminated thin sands better than that inverted P-imp section of original seismic. Slices of inverted P-imp are also generated between OCS & OCS-1, and OCS-2 & OCS-3 levels for both the inversion outputs. Slices of inverted P-imp, generated for above mentioned windows, using original seismic as well as CTT seismic are shown in Fig.17 & 18. From the slices of P-impedance (Fig.17-18) it is evident that the distribution of lithofacies within Kalol sand, KIX sand, Linch sand units, are better delineated in the P-imp slices of CTT seismic

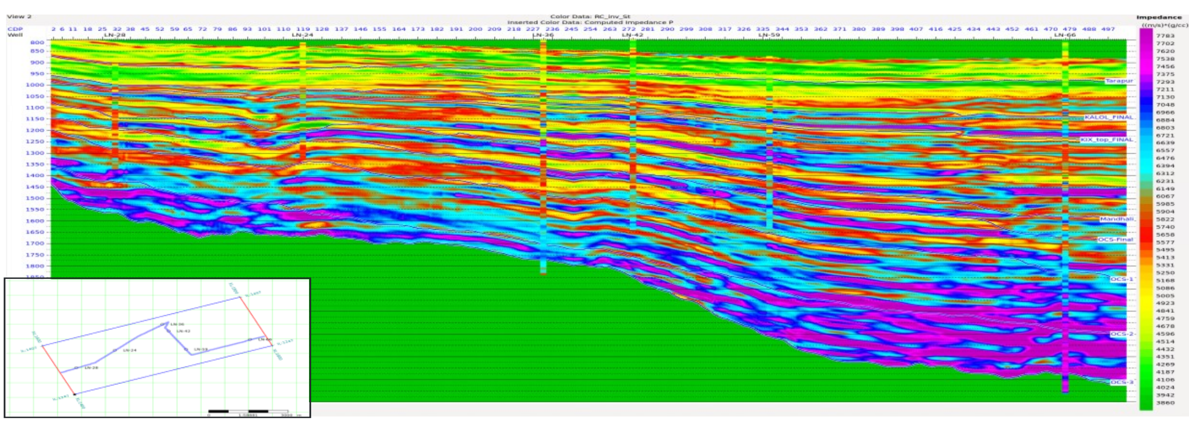

Fig. 15: Inverted impedance sections of original seismic.

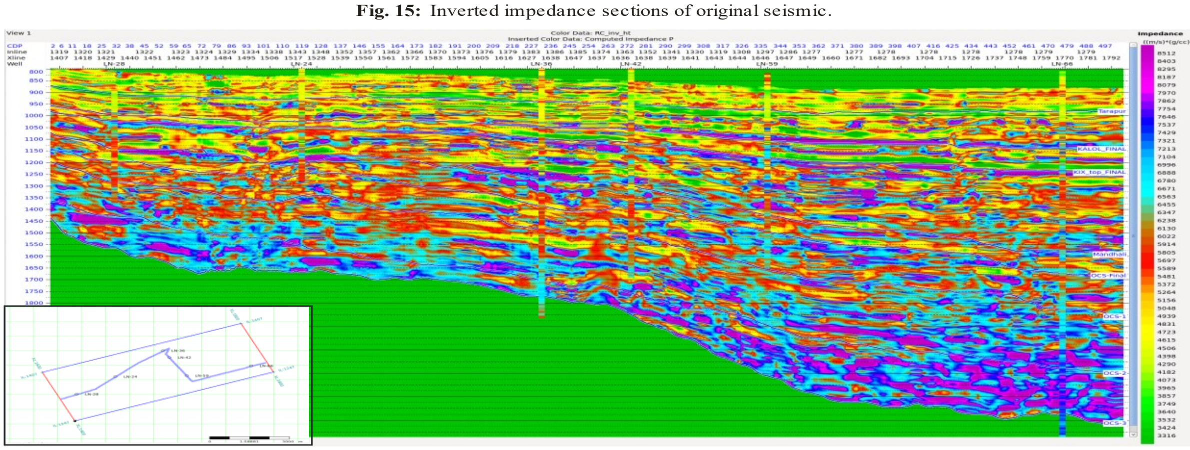

Fig. 16: Inverted impedance section of CTT seismic

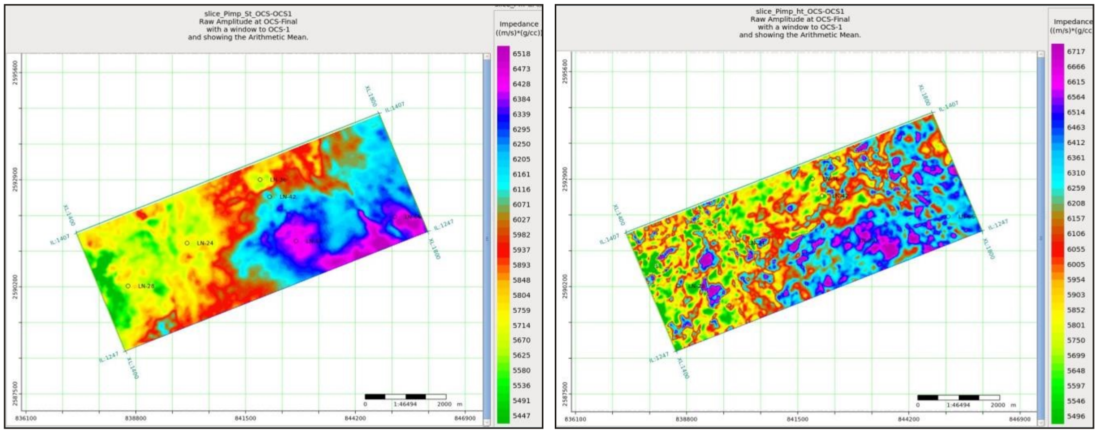

Fig. 17: Slice of inverted P-imp of original seismic (left) and CTT seismic (right) calculated within window of OCS-OCS1

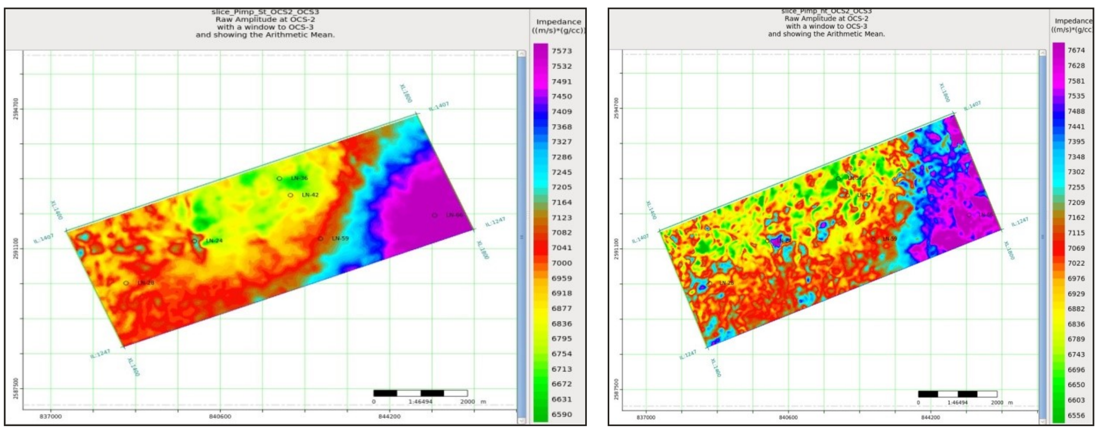

Fig. 18: Slice of inverted P-imp of original seismic (left) and CTT seismic (right) calculated within window of OCS2-OCS3.

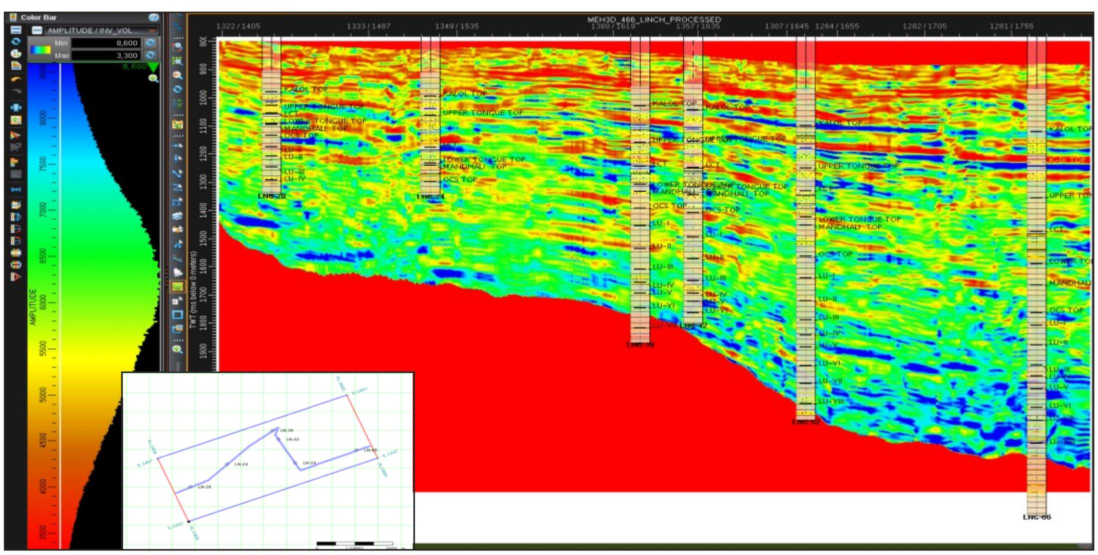

Fig. 19: Arbitrary line section of Inverted P-imp using CTT seismic passing through drilled wells overlain with lithologs.

in comparison to P-imp slices of original seismic. The resolvability is also improved.

Validation

Sections of inverted P-imp of CTT seismic overlain with lithologs, passing through drilled wells are shown in Fig. 19. The discrete and thin sand bodies within LU-I units having composite thickness of 4-11m have been encountered in the drilled wells LN-B, LN-C & LN-D, it is seen on the output section that these sand bodies are partially delineated and validated at the well locations. Also, the discrete and thin sand bodies within LU-III units having composite thickness of 2-16m which are encountered in the drilled wells LN-B, LN-C, LN-D & LN-E, are partially delineated and duly validated at the wells.
However, the deeper sand bodies within LU-IV units having composite thickness 6-12m, encountered in the drilled wells LN-C and LN-F, seems to be not validated in the output section.

Conclusion

Complex trace transform (CTT) is relatively new approach with a very sound theoretical background for improving S/N ratio and resolution ability of data. The frequency bandwidth of CTT seismic is increased significantly in comparison to that of original seismic. The attribute slices generated using CTT seismic with reference to Kalol top, KIX top and OCS surfaces, indicates that distribution of lithofacies are better delineated and resolvability is also improved. Results of this study validate the thin and discrete beds within LU-I & LU-III sand units encountered in the drilled wells.

References

Hakan Karsli1, DermanDondurur, and GünayÇifçi, Application of complex-trace analysis to seismic data for random-noise suppression and temporal resolution improvement, Geophysics, Vol. 71, No. 3, May-June, 2006, V79–V86.

James D. Robertson, and Henry H. Nogami, Complex seismic trace analysis of thin beds, Geophysics, Vol. 49, No. 4, April,1984, P. 344-352.

Robertson J.D. et al, Complex seismic trace attributes, 1988, TLE.

Taner M.T. et al, Complex trace analysis of seismic signal by Hilbert transform, 1979, Geophysics, Vol.44.

Widess, M. B., 1973, How thin is a thin bed?, Geophysics, 38, 1176–1180.

Acknowledgement

The authors express their sincere thanks to Shri Ashutosh Bhardwaj, ED-HOI-GEOPIC for providing the opportunity to work on the project. Authors are thankful to Shri Dhruvendra Singh, Head INTEG for his valuable suggestions during the course of study. The authors are also thankful to WON Basin group, especially, Sh. S. C. Malviya for providing technical input for the project. Thanks are due to ONGC management for allowing to publish the paper in SPG conference, JAIPUR-2017.

Views and opinions expressed in this paper are of authors only, not necessarily be that of ONGC.